CHARACTERISTICS OF HEAT TRANSFER IN THE REGION OF GAS INJECTION INTO A SUPERSONIC HIGH-TEMPERATURE GAS STREAM

F. G. Bakirov and Z. G. Shaikhutdinov

UDC 536.244:533.6.011.5

An experimental study was made of the heat transfer distribution during gas injection into the supersonic region of a Laval nozzle. The dimensionless parameters governing this process have been established as a result.

Recently researchers have become greatly interested in studying supersonic flow with transverse injection of a secondary gas. In some reports the gasdynamic aspects have been covered thoroughly enough but no data at all are given about the heat transfer, although such data are necessary for a complete solution of the problem. In this study the authors have attempted to fill that gap.

The methodology of the experimental part was described in [1]. The gist of the test procedure was to measure the heat transfer coefficient on the basis of the transient heating of a special probe, the latter comprising a long cylinder thermally insulated around its lateral surface and mounted into the channel wall. Such a cylinder was mounted with its end flush against the wall surface exposed to the gas stream. The temperature–time curve of a probe was measured with a thermocouple built into it at a distance x from the end face exposed to the gas stream. The heat transfer coefficient was then determined according to the formula

$$\frac{T(x,\ \tau)-T_0}{T_f-T_0}=\operatorname{erfc}\frac{x}{2\sqrt{a\tau}}-\exp\left(Hx+H^2a\tau\right)\times\operatorname{erfc}\left(\frac{x}{2\sqrt{a\tau}}+H\sqrt{a\tau}\right),\tag{1}$$

which had been derived from the solution to the problem of transient heating of a semiinfinitely long cylinder with boundary conditions of the third kind [2]. The same solution may be written in criterial form, namely

$$\theta=\operatorname{erfc}\frac{1}{2\sqrt{\mathrm{Fo}_x}}-\exp\left(\mathrm{Bi}_x+\mathrm{Bi}_x^2\mathrm{Fo}_x\right)\operatorname{erfc}\left(\frac{1}{2\sqrt{\mathrm{Fo}_x}}+\mathrm{Bi}_x\sqrt{\mathrm{Fo}_x}\right),\tag{2}$$

where

$$\theta=\frac{T(x,\ \tau)-T_0}{T_f-T_0};\tag{3}$$

$$H=\frac{\alpha}{\lambda};\qquad \mathrm{Bi}_x=\frac{\alpha x}{\lambda};\qquad \mathrm{Fo}_x=\frac{a\tau}{x^2}.\tag{4}$$

The length of such a thermally insulated rod was designed so as to prevent any temperature perturbation from reaching its unexposed end during the entire period.

For the experiment we had 30-40 such rod probes mounted into the nozzle wall throughout the gas injection zone. The thermocouple readings were recorded on model N-700 loop oscillographs. These thermocouples covered one half of the anticipated flow perturbation zone. Symmetrically, in the other half of the flow perturbation zone we measured the pressure field and, by such an arrangement, the heat transfer characteristics could be matched with the gasdynamic aspects of the flow pattern.

S. Ordzhonikidze Institute of Aviation, Ufa. Translated from Inzhenerno-Fizicheskii Zhurnal, Vol. 24, No. 5, pp. 790-797, May, 1973. Original article submitted August 7, 1972.

For the experiment we used supersonic conical nozzles with the Mach number equal to 2.75 or 3.36 in the plane of injection, all mounted on a gas generator. As the operating medium (both as the working gas and as the injected gas) we used the products of kerosene combustion in air at a stagnation temperature T_1^* ranging from 600 to 1700°K under a total pressure $P_1^* = 20$–43 bars. Gas was injected normally to the nozzle wall through a circular orifice 4-12 mm in diameter (d_2). This secondary gas for injection was supplied from the combustion chamber of the gas generator. The discharge rate of secondary gas was varied by changing the diameter d_2 of the injection orifice and by placing flow diaphragms in the supply pipe, as a result of which various modes of gas supply could be simulated: by pressure throttling or by varying the section area of the injection nozzle. The distance from the injection orifice to the throat of the main nozzle was such that the curved density jump preceding an injected jet did not form at the nozzle wall and that no reflected shock wave appeared as a result. The Reynolds number Re_1 varied from 10^6 to $8 \cdot 10^6$.

Highly significant to the final results of such a study is the choice of the characteristic temperature T_f, in this case the local temperature of the boundary layer in the perturbation zone of the gas stream – analogous to the recovery temperature T_e in a boundary layer. It is well known that this temperature depends on the degree of dissociation of the working gas, on the relative radiation intensity, on the conditions of heat transfer, etc. Under the conditions of our experiments there occurred almost no dissociation and the radiant thermal flux striking the nozzle wall constituted a negligible fraction of the total thermal flux here. A numerical analysis pertaining to such test conditions yielded a characteristic temperature T_f approximately 5-8% lower than T_1^*, i. e., $T_f \simeq (0.92-0.95)T_1^*$ and this value served as the basis for further analysis. Actual measurements of T_f yielded $T_f/T_1^* = (0.92-0.95) \pm 0.08$.

A typical profile of the relative heat transfer coefficient $\bar{\alpha} = \alpha/\alpha_0$ along a nozzle, $\bar{x} = x_1/d_2$, is shown in Fig. 1, for a pressure $P^* = 32$ bars and a ratio of stagnation temperatures $T_2^*/T_1^* = 0.95$ at three different relative flow rates of injected gas. An angular profile (central angle φ_1) of $\bar{\alpha}$ is shown in Fig. 2 for the same conditions across a transverse nozzle section.

The values of the heat transfer coefficient α measured during gas injection into a nozzle have been referred to the respective local values α_0 for the same nozzle with the same working gas stream measured under the same conditions but without injection. The choice of these α_0 values as the natural scale for α has helped to reduce the possible systematic error in this method of determining the heat transfer coefficient. Its values α_0 obtained without injection into the nozzle were then compared with values found by various methods of calculating it (by the formula for cylindrical pipes, by the Bartz, the Avduevskii, the Ievlev, or other methods) and the agreement was found satisfactory.

According to Figs. 1 and 2, within the injection zone the heat transfer pattern undergoes a major modification and the heat transfer rate increases at the entire nozzle surface bounded by the perturbation zone. In order to explain this, we compare the heat transfer characteristics with the pressure field data obtained in the same experiment.

A simultaneous analysis of these results and earlier published results pertaining to the physical interaction between streams during injection of gas into a supersonic stream [3, 4, et al.] has shown that the heat transfer coefficient passes through a local minimum on the separation line of the three-dimensional boundary layer (length s). This agrees closely with the conclusion in [5], where it has been suggested that the separation point of a boundary layer be determined on the basis of the minimum heat transfer coefficient α. The heat transfer coefficient is maximum on the diffluence line a ahead of the injected jet (Fig. 1). The results obtained agree closely with photographs taken by the Tepler method (see, e. g., [3]), where $\bar{\alpha}_{max}$ corresponds to the curved density jump occurring at the nozzle wall. Directly ahead of a jet the heat transfer coefficient decreases sharply, which has to do with the presence here of a stagnation zone. It is to be noted that a thermally insulated rod probe for determining the local heat transfer coefficients has finite dimensions and that this causes some averaging of the measured $\bar{\alpha}$ values. For a more accurate determination of $\bar{\alpha}_{max}$, therefore, into the injection nozzle were inserted special diaphragms with inside holes somewhat eccentric relative to the outer circumference, which made it possible to regulate – within the amount of this eccentricity – the location of the injection orifice in the nozzle wall relative to the fixed thermally insulated rod probes. The heat transfer coefficient increases also behind an injected jet. It is interesting to note that $\alpha \approx \alpha_0$ over the distance $\bar{x} = 8$ to 10, i. e., the perturbation almost ceases to affect the heat transfer here, and this indicates a regular flow within that zone. The angular variation of $\bar{\alpha}$, namely as a function of the central angle φ_1, duplicates the gasdynamic pattern: maxima of the heat transfer coefficient correspond to the diffluence lines and its minima correspond to the confluence lines in the oil-traced flow pattern.

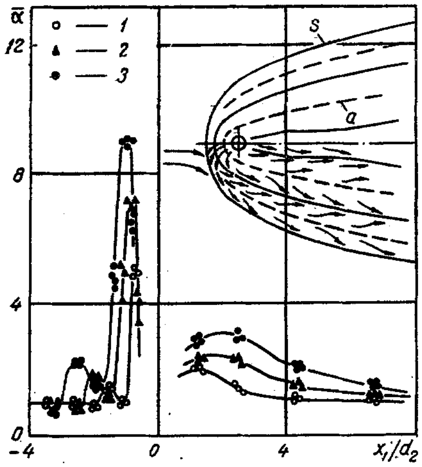

Fig. 1

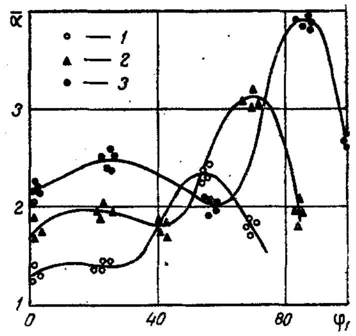

Fig. 2

Fig. 1. Variation of the heat transfer coefficient along a nozzle, during injection of a sonic jet through a circular orifice (d_2 = 10 mm, $Ma_1 = 2.75$): 1) $\overline{G}_2$ = 2.2%, 2) 4.75%, 3) 7.5%.

Fig. 2. Distribution of the heat transfer coefficient across the transverse nozzle section at $x_1/d_2 = 4.1$, where Ma_1 = 2.75, during gas injection: 1) $\overline{G}_2$ = 2.2%, 2) 4.74%, 3) 7.5%; φ_1 (deg).

Our experimental study concerning the effect of the various parameters of both the working and the secondary stream on the heat transfer rate within the perturbation zone has shown that $\overline{\alpha}$ is basically affected by the relative flow rate of the secondary gas $\overline{G}_2 = G_2/G_1$ and by the Mach number of the working stream Ma_1 in the injection plane. The stagnation pressure of the injected gas P_2^* at a constant flow rate, as well as the pressure P_1^* and the temperature T_1^* of the working stream, have almost no effect on the relative heat transfer coefficient $\overline{\alpha}$, neither does the shape of the working nozzle or the shape of the injection nozzle.

The maximum value of the heat transfer coefficient $\overline{\alpha}$ has been plotted in Fig. 3 as a function of the relative injection rate and as a function of the Mach number in the oncoming stream. It is quite evident here that the relative injection rate has a decisive effect on $\overline{\alpha}_{max}$. An increase in the Mach number also brings about some increase in the maximum heat transfer coefficient. This means that shifting the injection orifice in the nozzle wall closer toward the critical nozzle section would cause the maximum relative heat transfer coefficient $\overline{\alpha}_{max}$ to decrease somewhat, but its absolute value would increase together with the local relative heat transfer coefficient $\overline{\alpha}_0$.

In order to establish the governing parameters of the process under study, we will resort to dimensional analysis and thus reveal those dimensionless parameters without having to set up equations to describe the said process [6].

All independent parameters in this problem which describe the model phenomenon will be enumerated as follows, with the heat transfer coefficient α treated as the sought unknown quantity: coordinates of points in the nozzle x_1, φ_1, parameters of the working gas w_1, ρ_1, c_{p1}, λ_1, η_1, R_1, T_1, parameters of the injected gas w_2, ρ_2, c_{p2}, λ_2, η_2, R_2, T_2, nozzle diameter at a given section D_1, injection angle β, wall temperature T_w, acceleration of gravity g, nozzle aperture angle γ_1, distance from the critical section l_1, profile parameters Π_1 and Π_2 of the working nozzle and the injection nozzle respectively, diameter of the injection orifice d_2, scale factors of turbulence intensity l_T and ε, and discharge coefficient of the injection nozzle μ_2.

Thus, we have a set of 29 parameters which determine the heat transfer in the nozzle and in the perturbation zone during gas injection. The fundamental units will be here the kilogram (kg), the meter (m), the second (sec), and the degree Kelvin (°K).

The process will be regarded as quasisteady. We apply Buckingham's π theorem. The total number of dimensionless groups will be

$$r = n - m' = 29 - 4 = 25. \tag{5}$$

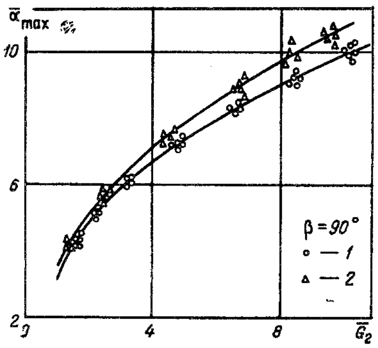

Fig. 3

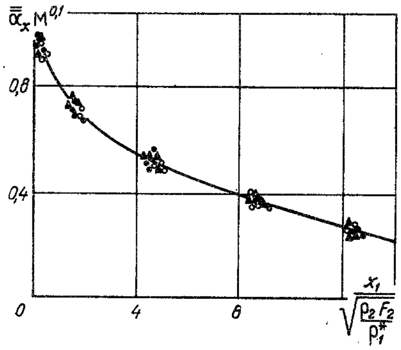

Fig. 4

Fig. 3. Maximum heat transfer coefficient $\bar{\alpha}_{max}$ ahead of an injected jet, as a function of the relative flow rate of the injected gas $\bar{G}$ (%): 1) $Ma_1 = 3.36$, 2) 2.75; $\beta = 90°$.

Fig. 4. Universal relation for the maximum heat transfer coefficient at a nozzle cross section behind the injection orifice.

One dimensionless quantity $\bar{\alpha}$ among them will be a function of 24 other dimensionless quantities. Continuing the dimensional analysis as in [6], we find that the solution to the problem of heat transfer during secondary injection of gas into the nozzle may, for example, be put in the following form:

$$Nu = f\left(\frac{x_1}{d_2}, \varphi_1, Re_1, Re_2, Pr_1, Pr_2, Fr, Ma_1, Ma_2, \gamma_1, \beta, k_1, k_2, \Pi_1, \Pi_2, \frac{l_1}{d_2}, \frac{l_T}{d_2}, \frac{D_1}{l_1}, \varepsilon, \mu_2, \frac{w_2}{w_1}, \frac{\rho_2 w_2^2}{\rho_1 w_1^2}, \frac{T_2^*}{T_1^*}, \frac{T_W}{T_1^*}\right). \quad (6)$$

In a more general formulation of the problem this set of dimensionless groups will also include the Strouhal number $Sh = \omega\tau_0/l$ with τ_0 denoting the characteristic time.

Evidently, the most general solution to the problem is extraordinarily complex in form. For simplification, therefore, it becomes necessary to examine each dimensionless group here as to its effect on the sought result, i. e., as though to establish coefficients which would characterize the effect of each of these parameters. In the lack of an analytical solution to the problem, naturally, the effect of each group on the process can only be found experimentally.

The test results revealing the effect of the dimensionless parameters in Eq. (6) on the relative heat transfer coefficient $\bar{\alpha}$ under given conditions ($\beta = 90°$, $Ma_2 = 1$, etc.), as well as other test data published in the technical literature, have made it possible to eliminate those parameters with respect to which the process is almost self-adjoint. The final solution for our specific case becomes then

$$\bar{\alpha} = f\left[\frac{x_1}{d_2}, \varphi_1, Ma_1, \frac{\rho_2 F_2}{\rho_1^* q(\lambda_1)\cdot 1_{area}}, \theta_W\right]. \quad (7)$$

Representing α by $\bar{\alpha} = \alpha/\alpha_0$ rather than in terms of the Nusselt number has to do with the fact that the relative heat transfer rate is almost self-adjoint with respect to the Reynolds number Re_1 over its test range, while $Nu = f(Re_1)$ and the use of $\bar{\alpha}$ instead appears thus logical. Besides, $\bar{\alpha}$ can also be expressed as

$$\overline{Nu} = \frac{Nu}{Nu_0} = \frac{\dfrac{\alpha l}{\lambda_1}}{\dfrac{\alpha_0 l}{\lambda_1}} = \bar{\alpha}. \quad (8)$$

The complex $\frac{\rho_2 F_2}{\rho_1^* q(\lambda_1)\cdot 1_{area}} = \frac{G_2}{\frac{G_1}{F_1}\cdot 1_{area}}$ represents the ratio of flow rates, the flow rate of injected gas to the flow rate of working gas, per unit area.

When $\beta \neq 90°$ and $Ma_2 \neq 1$, then the solution for the case of secondary gas supplied from the combustion chamber can be written in the form

$$\bar{\alpha} = f\left[\frac{x_1}{d_2},\ \varphi_1,\ \mathrm{Ma}_1, \mathrm{Ma}_2, \bar{q},\ \frac{x^*}{m_1 w_1} \cdot \frac{w_2}{w_1}(1-\cos\beta),\ \theta_w\right], \tag{9}$$

where $\bar{q} = (\rho_2\omega_2^2/\rho_1\omega_1^2)$, $\theta_w = (T_w/T_1^*)$, and $x^* = m_2\omega_2[(\omega_1/\omega_2) - \cos\beta]$; complex $(x^*/m_1\omega_1)\cdot(\omega_2/\omega_1)(1-\cos\beta)$ has been introduced earlier by B. S. Vinogradov and V. L Panchenko. This complex generalizes the effect of the dimensionless parameters β, k_1, k_2, Re_2, ω_2/ω_1, (R_2T_2/R_1T_1).

It must be noted that the set of groups in Eq. (6) can be obtained by a different method too, namely by an analysis of the equations for the working stream and the secondary stream. These equations include the conservation of total gas flow in the nozzle, of energy, and of momentum, the equation of state for the working gas and for the injected gas, etc.

Despite the great simplification achieved by expressing the solution to the problem in the form (7) rather than in the form (6), the representation of experimental results in the form (7) was found cumbersome, owing to the complexity of the $\bar{\alpha}$-field in the perturbation zone of the nozzle.

For this reason, we were able to derive relations of this kind only from data with a few typical values of $\bar{\alpha}$ in the perturbation zone and not the entire $\bar{\alpha}$-field.

In Fig. 3 are shown some data pertaining to the maximum relative heat transfer coefficient $\bar{\alpha}_{max}$ in the region ahead of an injected jet, with $Ma_2 = 1$ and $\beta = 90°$. These results can be approximated by the relation

$$\bar{\alpha}_{max} = 1 + \mathrm{Ma}_1^{0.35}\left[\frac{\rho_2 F_2}{\rho_1^* q(\lambda_1)\cdot 1_{area}} - 0.19\right]^{0.45}. \tag{10}$$

The location where $\bar{\alpha} = \bar{\alpha}_{max}$ occurs ahead of a jet is determined from the relation

$$\frac{x_m - \frac{d_2}{2}}{x_s - \frac{d_2}{2}} = 0.2\text{-}0.25, \tag{11}$$

with x_m denoting the coordinate of the point where $\bar{\alpha} = \bar{\alpha}_{max}$.

The maximum heat transfer coefficient in the perturbation zone at an arbitrary nozzle section behind the injection orifice is determined from the relation

$$\bar{\bar{\alpha}}_x = \left[0.98 - 0.224\left(\frac{x_1}{\sqrt{\frac{\rho_2 F_2}{\rho_1^*}}}\right)^{0.46}\right]\mathrm{Ma}_1^{-0.1} \tag{12}$$

which generalizes the experimental data for $x \geq 0$, $\beta = 90°$, and $Ma_2 = 1$ (see Fig. 4). Here $\bar{\bar{\alpha}}_x = \bar{\alpha}_x/\bar{\alpha}_{max}$ and $\bar{\alpha}_x$ is the maximum relative heat transfer coefficient at any nozzle section behind the injection orifice.

Relations (10) and (12) do not contain the parameter θ_w, because its effect has not been the concern of our study.

The relations derived can be useful in the design of thermal protection for nozzles with secondary injection, for the control of the draft vector.

NOTATION

α is the heat transfer coefficient;
x is the distance between the rod end exposed to the stream and any point in the body;
x_1 is the coordinate of a point on the nozzle surface, measured along the generatrix from the cross section through the center of the injection orifice;
φ_1 is the central angle between the generatrices of the nozzle surface through the center of the injection orifice and through any given point respectively;
τ is the time;
P is the pressure;
T is the temperature;
W is the velocity;
ρ is the density;
c_p is the specific heat at constant pressure;
m is the mass;

F	is the surface area;
G	is the gas flow rate per second;
a	is the thermal diffusivity;
λ	is the thermal conductivity;
η	is the dynamic viscosity;
D, d	are the diameters;
l	is the length;
R	is the gas constant;
k	is the adiabatic exponent;
β	is the injection angle;
γ	is the aperture angle of a conical nozzle;
r	is the total number of dimensionless groups;
n	is the total number of dimensionless parameters;
m'	is the number of independent units;
Re	is the Reynolds number;
Pr	is the Prandtl number;
Nu	is the Nusselt number;
Bi	is the Biot number;
Fo	is the Fourier number;
Fr	is the Froude number;
Sh	is the Strouhal number;
Ma	is the Mach number;

Subscripts

0	refers to initial values of parameters or their values without gas injection into the nozzle;
1	refers to parameters of the working gas;
2	refers to parameters of the secondary gas;
w	refers to parameters at the nozzle wall;
max	refers to maximum value;
e	refers to recovery values;
x	refers to values at any nozzle cross section;
asterisk*	refers to stagnation values.

LITERATURE CITED

1. N. M. Tsirel'man, F. G. Bakirov, and Z. G. Shaikhutdinov, Inzh. Fiz. Zh., 24, No. 2 (1973).
2. A. V. Lykov, Theory of Heat Conduction [in Russian], Izd. Vysshaya Shkola, Moscow (1967).
3. A. I. Glagolev et al., Izv. Akad. Nauk SSSR, Mekhan. Zhidk. i Gaza, No. 3 (1967).
4. D. M. Voitenko et al., Izv. Akad. Nauk SSSR, Mekhan. Zhidk. i Gaza, No. 1 (1966).
5. D. A. Needham, Rocket Engrg. and Cosmonautics [Russian translation], 3, No. 4 (1965).
6. A. A. Gukhman, Introduction to the Theory of Similarity [in Russian], Izd. Vysshaya Shkola, Moscow (1967).